ELSEVIER

Photodetachment of fullerene monoanions and dianions in a Penning trap: Probes of delayed electron emission and associated activation barriers

Bruno Concina [a],[1], Marco Neumaier [a], Oliver Hampe [a],[*], Manfred M. Kappes [a],[b]

[a] *Institut für Nanotechnologie, Forschungszentrum Karlsruhe, P.O. Box 3640, D-76021 Karlsruhe, Germany*
[b] *Institut für Physikalische Chemie, Universität Karlsruhe, Kaiserstr. 12, D-76128 Karlsruhe, Germany*

Abstract

Singly and doubly charged fullerene anions were introduced into gas phase by means of electrospray starting from a solution containing a very efficient electron donor compound. Following isolation and trapping, mass selected anions were irradiated with a ns-pulse from a Nd:YAG laser at the third harmonic ($h\nu = 3.5$ eV) in order to study (delayed) photoemission. We present results on the laser-fluence dependence of photoemission for singly charged C_{76}^- and C_{84}^- as well as for doubly charged C_{76}^{2-}. Results are discussed in terms of statistical electron emission as opposed to direct detachment. They are further analyzed to give information on the number of photons necessary to induce delayed electron emission on the experimental time scale. The averaged absolute absorption cross-sections obtained were about 0.6–0.8 Å^2 for all species probed. The agreement between experimental data and statistical modelling shows that electronic excitations which rapidly relax to vibrationally hot ions provide the dominant contributions to the 355 nm absorption cross-sections. As a corollary, we show that direct single-electron detachment is a minor process for the singly charged fullerene anions having a cross-section <0.02 Å^2. For C_{76}^{2-}, electron emission follows an absorption law in which single-photon excitation is the leading contribution. From the data we deduce a Coulomb barrier height for C_{76}^{2-} of 1.20 eV.
© 2006 Elsevier B.V. All rights reserved.

Keywords: Multianions; Fullerenes; Photodetachment; Thermionic emission; Clusters

1. Introduction

Delayed electron emission has been recognized as an important relaxation channel upon excitation of clusters and is often described in analogy to the well-known bulk phenomenon of thermionic emission. Experimentally, evidence for this particular electron emission mechanism is based on the characteristic time scale of the process and/or the specific (thermal) energy distribution of the emitted electrons. Excitation of the cluster of interest is typically achieved by thermal heating (e.g., using an oven source), electron attachment or – and most widely used – single or multiple photon absorption upon irradiation with lasers. Early accounts of delayed electron emission include pioneering studies on transition metal clusters [1,2] like photoelectron spectroscopic probes of small tungsten cluster anions [3–5] and lifetime measurements on multi-photon excited neutral niobium clusters [6]. Arguably, fullerenes comprise the most widely studied system in this context. Pioneering experiments on delayed ionization of neutral C_{60} and C_{70} after ns-laser multi-photon excitation were reported by Campbell et al. [7] and Wurz and Lykke [8]. For neutral and positively charged fullerenes, delayed ionization has typically been found to be in competition with fragmentation (=C_2 loss) due to comparable activation energies [9]—unless fs-laser excitation was employed [10]. The first observation of delayed emission from C_{60}^- was reported by the group of Smalley [11] and more systematically studied as a function of excitation energy (by means of surface collisions) by Yeretzian et al. [12]. Since the activation energy for electron loss from a negatively charged ion – namely the first adiabatic electron affinity of the corresponding neutral – is much smaller than the dissociation energy, the fragmentation channel is completely quenched.

More recently, it has become clear that an accurate description of delayed electron emission rates on time scales longer than ms

---

* Corresponding author.
E-mail address: Oliver.Hampe@int.fzk.de (O. Hampe).
[1] Present address: Laboratoire de Spectrométrie Ionique et Moléculaire, UMR 5579, CNRS and Université Lyon I, Bât. A. Kastler, 43 bd du 11 novembre 1918, F-69622 Villeurbanne cedex, France.

requires that radiative cooling is also adequately accounted for. In this context extensive effort has been put into probing the lifetime of (photo) excited fullerene anions using the Aarhus ion storage ring [13]. Observations included the finding that C_{60}^- radiates energy with an intensity of about 200 eV/s after (multiphoton) excitation to 14 eV. This was discussed in terms of low-lying electronically excited states which are populated at the corresponding effective temperature (1400 K) and which contribute to the overall radiative power [14].

In contrast to singly charged species, thermal emission of electrons from doubly or multiply charged anions – also termed multianions – is a relatively new field. Multianions pose new challenges/questions as to: (i) a proper description of the (non-local) repulsive Coulomb barrier to be overcome or tunnelled through upon electron emission, (ii) the possibility of thermally activated tunneling processes, (iii) the spectroscopic characterization of the ground and excited states involved, and (iv) the experimental generation of such multianions to begin with. Fullerene-dianion delayed electron emission was first reported by Compton et al. [15] after sequential attachment of two electrons to C_{84}. Lifetime measurements led to the inference of an effective activation barrier for electron loss of 2.18 eV. Upcharging upon few-eV electron attachment to monoanions stored in Penning traps [16–18] has been demonstrated to give (stable) dianions of various fullerene sizes C_n^{2-} ($n > 70$). An earlier study from our group established that electrosprayed room-temperature C_{70}^{2-} undergoes metastable decay with a half-life of 80 s [19]. Photoelectron spectroscopy probes (direct detachment) of doubly charged C_{76}^{2-} and C_{84}^{2-} revealed that the second electron affinities of these larger fullerenes are positive. Corresponding ground state Coulomb barrier heights of 1.1 and 0.95 eV were also inferred [20]. C_{60}^{2-} was already tentatively identified in early mass spectrometric probes [21,22]. However, only recently intense enough ion beams of this elusive species have been generated to allow further studies—via the expedient of keV collisions of C_{60}^- with sodium atoms [23]. As yet there has been no reported lifetime measurement of what is expected to be an electronically metastable dianion ground state.

In this contribution we report first results of photodetachment studies on singly and doubly charged fullerene anions C_{76} and C_{84} trapped in a FT-ICR mass spectrometer. We address questions regarding the prevalent electron emission mechanism after photo-excitation and provide quantitative results on power laws and associated activation energies.

2. Experimental

Studies were carried out using a Fourier transform ion cyclotron resonance mass spectrometer FT-ICR-MS (Apex II, Bruker Daltonics) equipped with a cylindrical Infinity® cell as described previously [24]. The fullerene samples C_{76} and C_{84} have been obtained by a high-performance liquid chromatography protocol developed in our laboratory [25] for enrichment of higher fullerenes starting with fullerene soot derived from a Kretschmar–Huffman type discharge oven. Fullerenes obtained in this way consist of a single isomer of C_{76} (D_2) whereas C_{84} comprises a 2:1 mixture of D_2(5) and D_{2d}(22)

isomers [26,27]. Negative ions of fullerenes were generated by electrospraying 0.1 mmol solutions of enriched C_{76} and C_{84} in 1,2-dichlorobenzene. As has been shown recently [19], the negative ion yield can be significantly enhanced by using tetrakis-dimethylaminoethylene (TDAE, Aldrich) as electron donor which was used as a 0.1 mol/l solution in toluene. In contrast to our earlier studies the fullerene and TDAE solutions were kept separate in two syringes and pumped independently at typical flow rates of 50 and 20 μl/h, respectively. They were mixed together in a T-like configuration (through 1/16 in. inner diameter PEEK tubings) just before entering the spraying needle (stainless steel, 200 μm inner diameter) held at a high voltage of typically −4500 V relative to the desolvation capillary. After spraying, ions were pretrapped in a hexapole trap for 0.1–0.3 s at about 10^{-3} mbar at ambient temperature. Efficient mass-selection to discriminate singly from doubly charged fullerene anions was achieved by using the high mass cut-off properties of multipole ion guides as a function of the applied rf voltage [28]. At an optimized value V_{p-p} of 70 V the discrimination between transmitted C_{76}^{2-} ($m/z = 456$) and blocked C_{76}^- ($m/z = 912$) was better than 4000:1.

The vibrational excitation of ions entering the ICR cell was estimated to be near room temperature. In order to allow ions to enter the trap the potential of the front trapping plate was pulsed open at a given delay. This time window allows a further pre-selection of ions of a certain mass/charge range due to their different time-of-flight between hexapole ion trap and ICR cell. Applied trapping voltages were typically −2 V. The ions were irradiated in the ICR cell by a single pulse from a Nd:YAG laser (30 Hz, third harmonic, 3.50 eV photon energy, 6 ns pulse length) as controlled by a computer-controlled mechanical shutter (Newport, Model 845 HP) as described recently [29]. The shutter is opened for 33 ms (=1/30 s) in order to allow a single laser pulse to be transmitted. This time defines an upper limit for the time delay between laser pulse and ion detection and is used in the simulations as the upper limit of the experimental time window (see below).[1] Individual mass spectra were recorded with and without laser in an alternating mode and this sequence was typically repeated 32 times yielding a signal-to-noise ratio on the parent ion of $>10^4$:1. The mass spectra were evaluated by integrating the ICR signals in the frequency domain and correcting for the charge state. They were then normalized to the respective parent ion signal of the reference mass spectrum without laser. We define the surviving fraction of parent ions as

$$S = \frac{I}{I_0} = \frac{[C_n^{(2)-}]^{\text{with laser}}}{[C_n^{(2)-}]^{\text{without laser}}} \tag{1}$$

In order to take power dependencies the laser beam was attenuated by means of a polarisation attenuator. For online measurements of the relative laser power we guided a reflection from a beam splitter onto a pyroelectric detector (33–140, Coherent) read out by a power monitor (Coherent, Fieldmaster GS).

---

[1] Ion intensities (and thereby the depletion) measured did not change as a function of the length of the transient recorded for detection; showing that there is no significant decay within the time window of the detection.
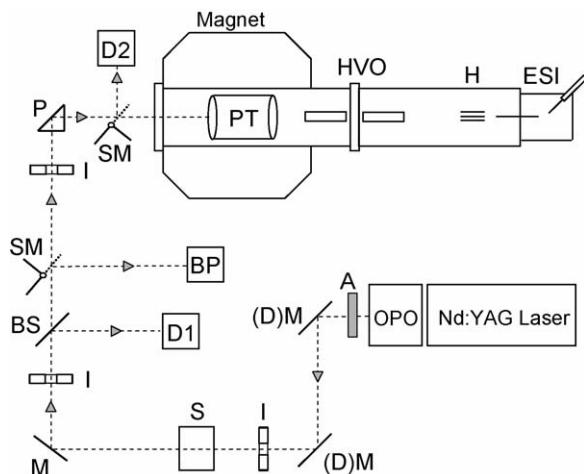
Fig. 1. Schematic of the experimental setup used for the photodetachment probes of ions trapped in a FT-ICR mass spectrometer. Electrospray ionization source (ESI) with hexapole trap (H), high-voltage ion transfer optics (HVO) and Penning trap (PT). A, attenuator; (D)M, dichroic mirror; I, iris; S, shutter; M, mirror; BS, beam splitter; SM, switchable mirror; P, prism; D_1 and D_2, laser power meter; BP, beam profiler.

The absolute laser power was measured in front of the FT-ICR entrance window using a thermopile detector (LM-10, Coherent) and correlated to the relative power measurement after each 32 pulse sequence. In order to determine the absolute laser fluence we also measured the beam profile and size by means of a CCD camera as implemented in a beam profiler (Beamstar V, Ophir). Gaussian envelopes were fitted over the recorded beam profiles and the full width at half-maximum of the Gaussians taken as the beam diameter. Finally the overlap between the laser beam (diameter of 6 mm FWHM) and ion cloud in the ICR cell was carefully optimized so as to give near-complete depletion at the maximum laser fluence (Fig. 1).

3. Results and discussion

Fig. 2 shows typical mass spectra of room-temperature electrosprayed C_{76}^{2-} parent ions before and after laser irradiation under otherwise identical conditions and without further scaling. We note that mass selection in the mass spectrum without laser (Fig. 2, top panel) is achieved by proper ion source conditions as described in the previous section and no further mass-selection in the ICR cell was employed since it typically impaired the overlap between laser and ion cloud as described recently [29].

As for all singly and doubly charged fullerene anions studied here, the loss of an electron is observed as the only m/z-changing relaxation process after photon absorption. Figs. 3 and 4 show the surviving fraction of singly charged C_{76}^- and C_{84}^- as a function of the absolute photon density at 355 nm. The data are analyzed on the basis of a (non-coherent) multi-photon absorption/delayed detachment mechanism in which the probability P to absorb k photons can be described by Poisson statistics which reads [29]:

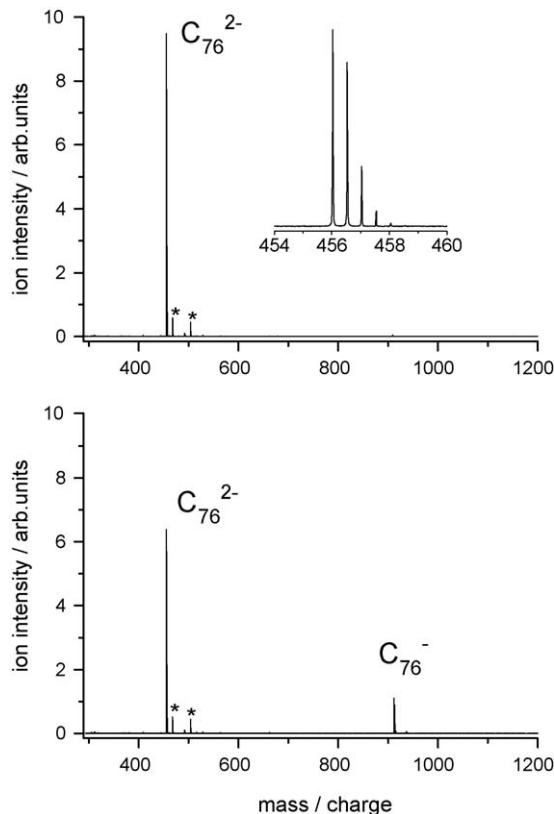$$P_k(F) = \frac{1}{k!}(\sigma F)^k e^{-\sigma F} \qquad (2)$$

Fig. 2. Top panel: Mass spectra from an electrosprayed C_{76}/TDAE solution with ion source conditions optimized for mass pre-selection to discriminate doubly from singly charged fullerene anions. Inset displays magnified portion of the dianion mass range indicating the half integer splitting of the isotopomers. Bottom panel: Same as above, but taken after irradiation with a 355 nm laser pulse (6 ns, 1 mJ/pulse). Peaks marked with an asterisk indicate small amounts of C_{78}^{2-} and C_{84}^{2-}.

Here F denotes the laser fluence (as the number of photons per unit area, Å^{-2}) and σ describes the apparent absorption cross-section which is assumed to be the same for all k photons. Decay is assumed to occur if the number of absorbed photons is equal to or larger than a critical number n. The absorption law describing the surviving fraction S of parent ions corresponding to such a
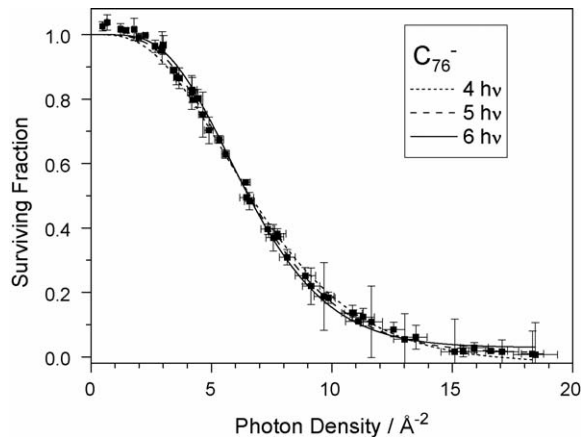

Fig. 3. Laser fluence dependence of photodetachment of C_{76}^- at 355 nm. Superimposed (solid line) is a data analysis based on Poisson statistics for multiple photon absorption (see Eq. (3) in the text and Table 1 for fit parameters).

Table 1
Optimized parameters (cross-section σ_{fit} and overlap α_{fit}) obtained from a Poisson statistics fit (Eq. (3)) to the data sets

n	σ_{fit} (Å^2)	α_{fit}	χ^2	σ (Å^2)	EA$_1$ (eV)[a]	EA$_2$ (eV)[b]
C$_{76}{}^-$						
4	0.55	1.02	7.8	**0.80 ± 0.20**	2.89 ± 0.05	
5	**0.72**	**0.99**	**3.4**	**0.80 ± 0.20**	2.89 ± 0.05	
6	**0.88**	**0.97**	**3.1**	**0.80 ± 0.20**	2.89 ± 0.05	
7	1.04	0.96	4.6	**0.80 ± 0.20**	2.89 ± 0.05	
C$_{84}{}^-$						
5	0.62	0.98	1.4	**0.75 ± 0.11**	3.14 ± 0.06	
6	**0.75**	**0.97**	**0.6**	**0.75 ± 0.11**	3.14 ± 0.06	
7	0.88	0.97	1.5	**0.75 ± 0.11**	3.14 ± 0.06	
C$_{76}{}^{2-}$						
1	**0.64**	**0.97**	**1.7**	**0.64 ± 0.10**		0.08 ± 0.17
2	1.27	0.97	35.1	**0.64 ± 0.10**		0.08 ± 0.17

χ^2 measure the goodness of the fits. Best fits are given in bold. The fit error on the cross-section σ_{fit} and the overlap α_{fit} is about 0.5%. The (average) cross-section σ is deduced from the best fit. Total error on σ is estimated to be 15% mainly due to variations in the laser beam profile.
  [a] Adiabatic first electron affinities taken from Ref. [33].
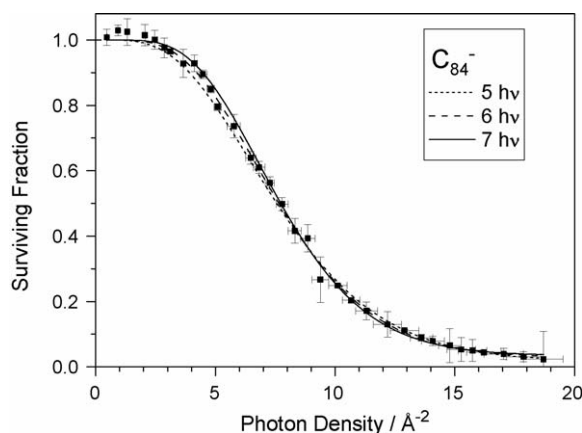 [b] Adiabatic second electron affinities taken from Ref. [20].

Fig. 4. Laser fluence dependence of photodetachment of C$_{84}{}^-$ at 355 nm. Superimposed (solid line) is a data analysis based on Poisson statistics for multiple photon absorption (see Eq. (3) in the text and Table 1 for fit parameters).

n-photon process can then be written as:

$$S_n(F) = (1 - \alpha) + \alpha \sum_{k=0}^{n-1} P_k(F) \qquad (3)$$

The overlap is taken into account by the parameter α ranging from 0 (no overlap) to 1 (complete overlap). Eq. (3) is used to fit the experimental data with σ and α being free fit parameters for any given n. The results are summarized in Table 1: the best fits, characterized by the lowest χ^2, are given in bold face. The experimental data points and the fits for a selection of n-values are shown in Fig. 3 (C$_{76}{}^-$), Fig. 4 (C$_{84}{}^-$) and Fig. 5 (C$_{76}{}^{2-}$). Best fits are given as solid lines. For C$_{76}{}^-$, $n = 5$ and 6 give rise to equivalent fits, as their respective χ^2 differs by less than 10%. For C$_{84}{}^-$, the number n of photons required to induce electron emission is 6. The dianion C$_{76}{}^{2-}$ shows a very different behaviour as shown in Fig. 5. Here, a one-photon process is clearly prevalent.

The analysis also leads to the determination of absolute cross-sections: 0.81 ± 0.20 Å^2 for C$_{76}{}^-$ 0.75 ± 0.11 Å^2 for C$_{84}{}^-$ and

0.64 ± 0.10 Å^2 for C$_{76}{}^{2-}$ These cross-sections can be understood as averages over the respective n photon absorption process in the case of the singly charged ions. The error on these measurements stems mainly from the variation of the laser beam profile (and also from the uncertainty in the value of n for C$_{76}{}^-$). While these cross-sections do not show a clear size-dependence, a charge dependence may be inferred for C$_{76}{}^{2-}$/C$_{76}{}^-$, with the apparent cross-section being somewhat smaller for the dianion than for the monoanion. Both monoanion measurements show a pronounced plateau at small photon densities, i.e., $S > 0.97$ for $F < 2$ Å^{-2}. This implies that the direct (one-photon) photoemission process is a minor channel (otherwise a fluence dependence like that of the dianion would be observed) and we infer an upper limit of 0.02 Å^2 for the associated cross-section. Apparently at this wavelength most of the oscillator strength is associated with multi-electron excitations of the anions—possibly dominated by the low-energy tails of the corresponding surface plasmon excitations of the fullerenes. A more detailed discussion on the apparent cross-sections compared to known solution phase
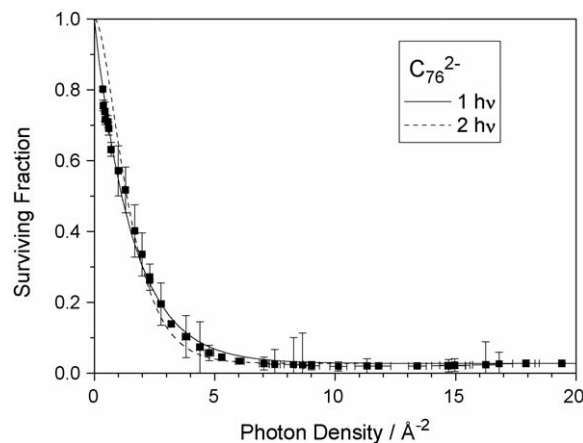

Fig. 5. Laser fluence dependence of photodetachment of C$_{76}{}^{2-}$ at 355 nm. Superimposed (solid lines) is a data analysis based on Poisson statistics for $n = 1$ and 2 (see Eq. (3) in the text and Table 1 for fit parameters).

UV–vis spectra [30] as well as on the type of electronic excitation involved will be given elsewhere [31].The clear multi-photon behaviour found for $C_{76}{}^-$ and $C_{84}{}^-$ suggests that the electron emission for monoanions can be described by a statistical (thermionic) process rather than a direct single-electron ionization step, although the photon energy used (3.50 eV) exceeds the ionization threshold (=first electron affinity) for both ions (see Table 1). The rate of statistical electron emission from a hot molecule may be described by the following equation [14]:

$$k(T) = \nu \exp\left(-\frac{E_b}{k_B T_e}\right) \qquad (4)$$

E_b is the activation energy, which for the singly charged anions is equivalent to the adiabatic electron affinity and T is the initial temperature before emission. The temperature T is obtained from the internal energy E after photon absorption $(E(T) = E_{\text{initial}}(300\,\text{K}) + nh\nu)$ using the vibrational density of states as described in Ref. [17] based on the concept of a microcanonical temperature. For C_{76}, e.g., $E_{\text{initial}}(300\,\text{K})$ amounts to 0.76 eV. T_e is the effective emission temperature corresponding to an effective heat-bath correction $(E(T_e) = E(T) - E_b/2)$.[2] The pre-exponential factor ν in Eq. (4) can be calculated from a consideration of detailed balance. If one assumes an average (energy independent) electron attachment cross-section σ_a, the pre-exponential factor takes the form:

$$\nu = \frac{m}{\pi^2 \hbar^3} \frac{g_f}{g_i} \sigma_a (k_B T_f)^2 \qquad (5)$$

m is the electron mass and g_f/g_i denotes the ratio between electron degeneracies in the final and initial states. T_f is the corresponding temperature after electron emission as obtained via $E(T_f) = E(T) - E_b$. We use ν values for the singly charged fullerenes based on the ν value derived from lifetime measurements on hot $C_{60}{}^-$ ($\nu = 2.1 \times 10^6 (T_f/\text{K})^2\,\text{s}^{-1}$) [14] scaled linearly for the higher number of atoms. Note that on the time scale of our experiment radiative cooling can be expected to substantially modify the decay times for excitation levels corresponding to temperatures above 1000 K. The effect of radiative cooling is therefore taken into account in this work as outlined by the Aarhus group [14] where it was found that the radiative intensity scales with T^6 and takes on a value of $I_r = 138$ eV/s at $T = 1356$ K for C_{60}.

The results are shown for $C_{76}{}^-$ and $C_{84}{}^-$ in Figs. 6 and 7, respectively. For comparison the time-dependent surviving fractions S_n are displayed for each n-photon process with and without the effect of radiative cooling. In the case of $C_{76}{}^-$ absorption/heating by five photons is required to induce (near-complete) electron emission even when accounting for radiative cooling. This is in good agreement with our experimental evaluation of $n = 5$ (or 6). For $C_{84}{}^-$ the electron emission following the absorption of six photons is severely inhibited by radiative
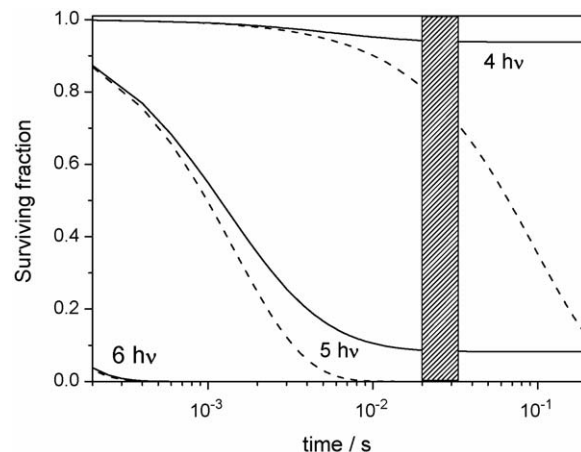

Fig. 6. Model calculation for statistical electron emission from $C_{76}{}^-$ (heated by n 355-nm photons) with (solid line) and without (dashed line) radiative cooling. The shaded area marks the experimental time window.

cooling: about two-thirds of the ions would survive. In contrast, absorption of seven photons leads to complete electron loss in spite of parallel radiative cooling. Again the agreement between experiment ($n = 6$) and the statistical modelling is good—given the fairly crude assumptions made in the experimental evaluation as well as in the model description.

To summarize this paragraph: electronic excitation of singly charged fullerene anions by a ns-laser at 355 nm is governed by (delayed) electron emission as the leading relaxation channel—as the observed laser power dependence is consistent with the predictions of statistical rate modelling (including radiative cooling) to within experimental error. This description is based on parameters that have been well established experimentally, namely the pre-exponential factor (=effective electron attachment cross-section) and the activation energy (=electron affinity).

For the doubly charged fullerene $C_{76}{}^{2-}$ one might then in turn wonder whether it is possible to deduce an activation energy from our experimental observations—assuming that a similar excitation/de-excitation mechanism applies. Unfortu-
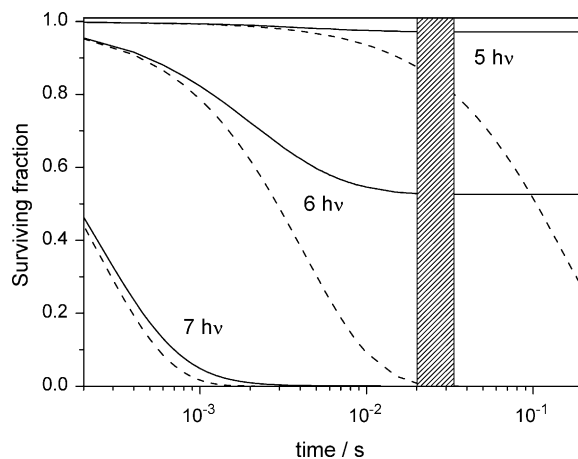

Fig. 7. Model calculation for statistical electron emission from $C_{84}{}^-$ (heated by n 355 nm-photons) with (solid line) and without (dashed line) radiative cooling. The shaded area marks the experimental time window.

---

[2] Note that this description is more general but equivalent to the heat-bath correction of the form $T_e = T - E_b/2C$ as long as the heat capacity C is constant which is a good approximation for temperatures $T > 1000$ K. For smaller temperatures the heat capacity becomes explicitly temperature dependent and we use the expressions from Ref. [17].
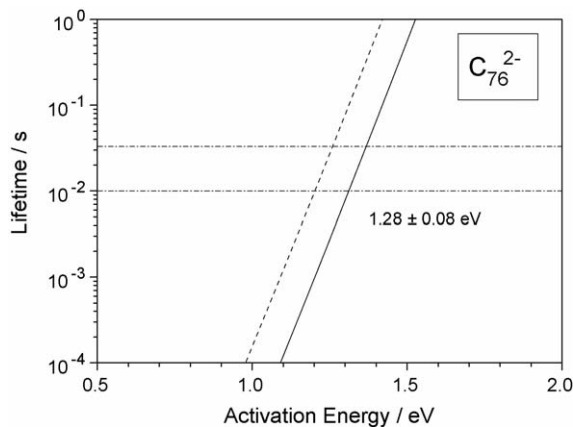
Fig. 8. Calculated lifetimes for statistical electron emission from C_{76}^{2-} for two different electron attachment cross-sections $\sigma_a = \pi R^2$ of 113 Å^2 (solid) and 11 Å^2 (dashed). The two horizontal lines mark the limits to the experimental time window. The correspondingly assigned activation energy amounts to 1.28 ± 0.08 eV.

nately, there are only rough estimates for the electron detachment/attachment cross-sections pertaining to doubly charged fullerene anions/monoanions. These range between 1 and 100 Å^2 [15,17]. It has been suggested that the radius at which the Coulomb barrier is maximal can be considered as an upper limit to the electron capture radius for the monoanion. Accordingly, we insert a value of $R = 6$ Å ($\sigma_a = \pi R^2 = 113$ Å^2) for C_{76}^{2-} [17] and calculate the expected lifetime as a function of the activation energy E_b using the statistical formalism given in Eqs. (4) and (5). Note that at this excitation energy, radiative cooling is likely negligible. Fig. 8 shows the calculated lifetime adopting the one-photon-absorption law described above (Fig. 5). From the upper limit of our experimental time window we then infer an upper bound to the activation energy of 1.35 eV.

A lower bound of 1.20 eV is obtained under the dual assumptions of a 10-fold smaller electron attachment cross-section ($\sigma_a = 11$ Å^2) and the lower limit of the experimental time window. We therefore assign a preferred value of 1.28 ± 0.08 eV. Physically, this activation energy likely corresponds to the Coulomb barrier (for an electron approaching the monoanion) augmented by the second electron affinity. Taking our value of the activation energy and subtracting from it EA$_2$(C$_{76}$) of 0.08 eV gives a Coulomb barrier of 1.20 eV. Within experimental error, this number is in excellent agreement with a previously reported value of 1.10 ± 0.2 eV obtained from a photoelectron spectroscopic study of C_{76}^{2-} [20]. It is somewhat smaller than the barrier (1.46 ± 0.3 eV) derived from an energy-resolved study of electron transfer collisions between C_{76}^{2-} and SF$_6$ [32].

4. Summary

Photodetachment studies on singly and doubly charged fullerene anions stored in a Penning trap are presented as a function of laser fluence. Assuming a multi-photon absorption law with equal cross-sections for the sequential steps, the experimental data yield the number of photons required to induce electron emission. The data are analyzed by contrasting to a statistical

electron emission rate model which is in good agreement for the singly charged ions for which the crucial activation energy, i.e., the first electron affinity, is well-known. This corresponds to a picture in which the electronically excited anion quickly decays into the vibrational manifold of the electronic ground state leading to electron emission from a "hot" molecular ion. Applying the same model assumptions to doubly charged C_{76}^{2-} we obtain a value for the Coulomb barrier of 1.2 ± 0.1 eV.

References

[1] T. Leisner, K. Athanassenas, D. Kreisle, E. Recknagel, O. Echt, J. Chem. Phys. 99 (1993) 9670.
[2] B.A. Collings, A.H. Amrein, D.M. Rayner, P.A. Hackett, J. Chem. Phys. 99 (1993) 4174.
[3] H. Weidele, D. Kreisle, E. Recknagel, G. Schulze Icking-Konert, H. Handschuh, G. Ganteför, W. Eberhardt, Chem. Phys. Lett. 237 (1995) 425.
[4] G. Ganteför, W. Eberhardt, H. Weidele, D. Kreisle, E. Recknagel, Phys. Rev. Lett. 77 (1996) 4524.
[5] J.C. Pinaré, B. Baguenard, C. Bordas, M. Broyer, Phys. Rev. Lett. 81 (1998) 2225.
[6] A. Amrein, R. Simpson, P. Hackett, J. Chem. Phys. 95 (1991) 1781.
[7] E.E.B. Campbell, G. Ulmer, I.V. Hertel, Phys. Rev. Lett. 67 (1991) 1986.
[8] P. Wurz, K. Lykke, J. Phys. Chem. 96 (1992) 10129.
[9] P. Weis, L. Rockenberger, R.D. Beck, M.M. Kappes, J. Chem. Phys. 104 (1996) 3629.
[10] E.E.B. Campbell, K. Hansen, K. Hoffmann, G. Korn, M. Tchaplyguine, M. Wittmann, I.V. Hertel, Phys. Rev. Lett. 84 (2000) 2128.
[11] L.-S. Wang, J. Conceicao, Ch. Jin, R.E. Smalley, Chem. Phys. Lett. 182 (1991) 5.
[12] C. Yeretzian, K. Hansen, R.L. Whetten, Science 260 (1993) 652.
[13] For a recent review see:
J.U. Andersen, E. Bonderup, K. Hansen, J. Phys. B: At. Mol. Opt. Phys. 35 (2002) R1, and references therein.
[14] J.U. Andersen, P. Hvelplund, S.B. Nielsen, U.V. Pedersen, S. Tomita, Phys. Rev. A 65 (2002) 053202.
[15] R.N. Compton, A.A. Tuinman, C.E. Klots, M.R. Pederson, D.C. Patton, Phys. Rev. Lett. 78 (1997) 4367.
[16] A. Herlert, R. Jertz, J.A. Otamendi, A.J.G. Martinez, L. Schweikhard, Int. J. Mass Spectrom. 218 (2002) 217.
[17] J. Hartig, M.N. Blom, O. Hampe, M.M. Kappes, Int. J. Mass Spectrom. 229 (2003) 93.
[18] A. Lassesson, N. Walsh, F. Martinez, A. Herlert, G. Marx, L. Schweikhard, Eur. J. Phys. D 34 (2005) 73.
[19] O. Hampe, M. Neumaier, M.N. Blom, M.M. Kappes, Chem. Phys. Lett. 354 (2002) 303.
[20] O.T. Ehrler, F. Furche, J.M. Weber, M.M. Kappes, J. Chem. Phys. 122 (2005) 094321.
[21] P.A. Limbach, L. Schweikhard, K.A. Cowen, M.T. McDermott, A.G. Marshall, J.V. Coe, J. Am. Chem. Soc. 113 (1991) 6795.
[22] R.L. Hettich, R.N. Compton, R.H. Ritchie, Phys. Rev. Lett. 67 (1991) 1242.
[23] B. Liu, P. Hvelplund, S.B. Nielsen, S. Tomita, Phys. Rev. Lett. 92 (2004) 168301.
[24] M.N. Blom, O. Hampe, S. Gilb, P. Weis, M.M. Kappes, J. Chem. Phys. 115 (2001) 3690.
[25] F.H. Hennrich, R.H. Michel, A. Fischer, S. Richard-Schneider, S. Gilb, M.M. Kappes, D. Fuchs, M. Burk, K. Kobayashi, S. Nagase, Angew. Chem. Int. Ed. 35 (1996) 1732.
[26] K. Kikuchi, N. Nakahara, T. Wakabayashi, S. Suzuki, H. Shiromaru, Y. Miyake, K. Saito, I. Ikemoto, M. Kainosho, Y. Achiba, Nature 357 (1992) 142.
[27] D.E. Manopoulos, P.W. Fowler, R. Taylor, H.W. Kroto, D.R.M. Walton, J. Chem. Soc. Faraday Trans. 88 (1992) 3117.

[28] D. Gerlich, in: Ch.-Y. Ng, M. Baer (Eds.), Advances in Chemical Physics, vol. LXXXII, John Wiley and Sons Inc., 1992.

[29] M. Kordel, D. Schooss, S. Gilb, M.N. Blom, O. Hampe, M.M. Kappes, J. Phys. Chem. A 108 (2004) 4830.

[30] R. Bauernschmitt, R. Ahlrichs, F.H. Hennrich, M.M. Kappes, J. Am. Chem. Soc. 120 (1998) 5052.

[31] O. Hampe, B. Concina, M. Neumaier, M.M. Kappes, in preparation.

[32] N. Neumaier, O. Hampe, M.M. Kappes, J. Chem. Phys. 123 (2005) 074318.

[33] O.V. Boltalina, E.V. Dashkova, L.N. Sidorov, Chem. Phys. Lett. 256 (1996) 253.